ACS APPLIED MATERIALS & INTERFACES

Research Article

www.acsami.org

Micro- and Nanoscale Energetic Materials as Effective Heat Energy Sources for Enhanced Gas Generators

Sang Beom Kim,[†] Kyung Ju Kim,[†] Myung Hoon Cho,[†] Ji Hoon Kim,[†] Kyung Tae Kim,[‡] and Soo Hyung Kim*[,†,§]

[†]Department of Nano Fusion Technology, College of Nanoscience and Nanotechnology, Pusan National University, 30 Jangjeon-dong, Geumjung-gu, Busan 609-735, Republic of Korea

[‡]Powder & Ceramic Division, Korean Institute of Materials and Science, 797 Changwon-daero, Seongsan-gu, Changwon-si, Gyeongnam 642-731, Republic of Korea

[§]Department of Nano Energy Engineering, College of Nanoscience and Nanotechnology, Pusan National University 30 Jangjeon-dong, Geumjung-gu, Busan 609-735, Republic of Korea

Supporting Information

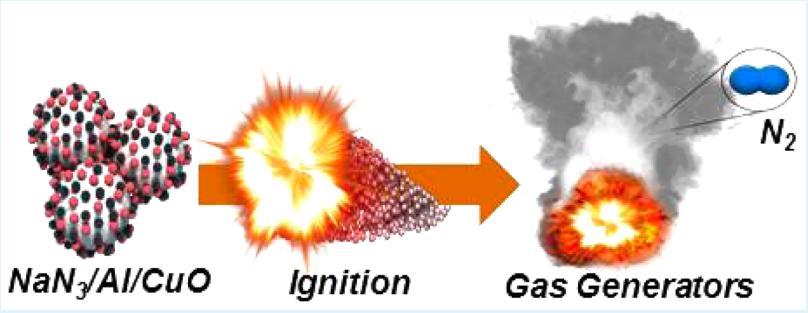

ABSTRACT: In this study, we systematically investigated the effect of micro- and nanoscale energetic materials in formulations of aluminum microparticles (Al MPs; heat source)/aluminum nanoparticles (Al NPs; heat source)/copper oxide nanoparticles (CuO NPs; oxidizer) on the combustion and gas-generating properties of sodium azide microparticles (NaN_3 MPs; gas-generating agent) for potential applications in gas generators. The burn rate of the NaN_3 MP/CuO NP composite powder was only ~0.3 m/s. However, the addition of Al MPs and Al NPs to the NaN_3 MP/CuO NP matrix caused the rates to reach ~1.5 and ~5.3 m/s, respectively. In addition, the N_2 gas volume flow rate generated by the ignition of the NaN_3 MP/CuO NP composite powder was only ~0.6 L/s, which was significantly increased to ~1.4 and ~3.9 L/s by adding Al MPs and Al NPs, respectively, to the NaN_3 MP/CuO NP composite powder. This suggested that the highly reactive Al MPs and NPs, with the assistance of CuO NPs, were effective heat-generating sources enabling the complete thermal decomposition of NaN_3 MPs upon ignition. Al NPs were more effective than Al MPs in the gas generators because of the increased reactivity induced by the reduced particle size. Finally, we successfully demonstrated that a homemade airbag with a specific volume of ~140 mL could be rapidly and fully inflated by the thermal activation of nanoscale energetic material-added gas-generating agents (i.e., NaN_3 MP/Al NP/CuO NP composites) within the standard time of ~50 ms for airbag inflation.

KEYWORDS: *aluminum particles, sodium azide, aluminothermic reaction, combustion, gas generator, airbag inflation*

1. INTRODUCTION

Energetic materials are mixtures of fuel and oxidizing materials that rapidly release heat and gas byproducts when ignited by external energy input.[1−4] The amount of thermal energy generated by energetic materials depends on the interfacial contact area and degree of intermixing between the fuel and oxidizing materials, the chemical compositions, and the size of the reacting materials.[5−9] In most formulations, macro- and microscale Al as a highly reactive and readily available material is used for the fuel materials, and various low-cost metal oxides (e.g., Fe_2O_3, $KMnO_4$, CuO, MoO_3) are used for energetic oxidizers.[10−16]

A gas generator burns fuels and oxidizers to produce large amounts of gas at lower temperatures without specific activation impulses.[17,18] The relatively low temperature allows the generated gas to be used in various applications, including powering turbo pumps in rocket motors and inflating airbags in automobiles. The gas-generating materials installed in gas generators thermally decompose into gases and residual metal composite materials upon ignition and thermal reactions. After the thermal decomposition of the gas-generating materials, the

Received: January 4, 2016
Accepted: March 23, 2016
Published: March 23, 2016

DOI: 10.1021/acsami.6b00070
ACS Appl. Mater. Interfaces 2016, 8, 9405−9412

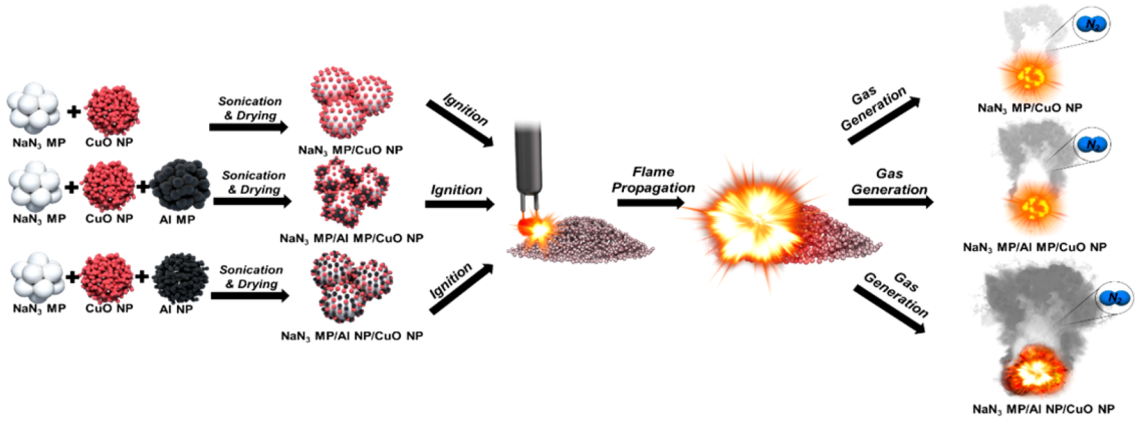

Figure 1. Schematics of fabricating NaN_3/Al/CuO composites and loading composites into the gas generator for airbag inflation by tungsten hot-wire ignition.

residual metal composite materials are stabilized by reactive coupling with various oxidizing agents.

Conventional gas generators employ various gas-generating materials such as sodium azide (NaN_3),[19−22] nitroguanidine ($CH_4N_4O_2$),[23,24] and tetrazole (CH_2N_4)[25−27] mixed with various metal oxides of copper oxide (CuO),[28] iron oxide (Fe_2O_3),[29] and potassium nitrate (KNO_3)[30,31] in ratios that produce the desired reaction rates and gas volumes.[32,33] However, when the heat generated is insufficient, the desired gas volume is not fully evolved because of the incomplete thermal decomposition of the gas-generating materials. This can cause serious malfunctions in gas-generating systems. To provide sufficiently high temperature for the thermal decomposition of the gas-generating materials, many studies have been performed on the use of various propellants, oxidants, and additives in the gas-generating material formulations.[34,35]

In this work, we examine the effects of the presence and size of Al particles on the gas-generating performance of NaN_3/CuO composite powders. Highly reactive Al, CuO, and NaN_3 were employed as the fuel materials, strong oxidizers, and gas-generating agents, respectively. Specifically, microparticles (MPs) and nanoparticles (NPs) of Al were added as fuel to the NaN_3 MP/CuO NP composites to observe the combustion and gas-generating characteristics when ignited. Finally, a small homemade airbag system was designed to examine the effective operation of a gas generator installed with the NaN_3/CuO/Al composite materials.

2. EXPERIMENTAL SECTION

NaN_3 MPs (gas-generating agent; Sigma-Aldrich) with average diameter of ∼75 μm (Figure S1a in the Supporting Information), and CuO NPs (oxidizer; NT Base, Inc.) with average diameter of ∼100 nm (Figure S1b) were employed. Al NPs (fuel; Nanotechnology, Inc.) with average diameter of ∼80 nm (Figure S1c) and oxide layer thickness of 7 nm (Figure S2a), and Al MPs (fuel; NT Base, Inc.) with average diameter of ∼10 μm (Figure S1d) and oxide layer thickness of 12 nm (Figure S2b) were also employed.

Figure 1 shows the schematics of fabricating the NaN_3 MP/CuO NP composite powders with the addition of Al MPs and Al NPs. NaN_3 was the gas-generating agent, decomposing into N_2 gas and Na products when heated to ∼350 °C. Al and CuO were used as the fuel and oxidizer for supplying heat energy for sufficient thermal decomposition of the gas-generating agents (i.e., NaN_3).

Three different composite powders of NaN_3 MP/CuO NP, NaN_3 MP/Al MP/CuO NP, and NaN_3 MP/Al NP/CuO NP were fabricated by sonication and drying processes. We performed a series of ignition tests for various mixing ratios of NaN_3/Al/CuO reactants. For the ignition tests, the mixing ratio of Al and CuO was always kept with Al:CuO = 30:70 wt % because it was the optimized mixing ratio for effectively generating heat energy when ignited.[7,8,13] Specifically, we observed that the composites were not stably ignited in the cases of NaN_3:Al:CuO = 90:3:7 and 83:5:12 wt %. When the mixing ratio was reached to a NaN_3:Al:CuO = 77:7:16 wt %, the composite was started to be stably ignited and actively generate gas byproducts. Thus, the mixing ratio of reactants was fixed to a NaN_3:Al:CuO = 77:7:16 wt % in this study. Each reactant was mixed in ethanol solution for 30 min using ultrasonication at 170 W and 40 kHz. These prepared composite powder samples were then dried in a convection oven for 30 min at 80 °C. After fabricating each composite powder, the sample was installed in a homemade gas generator with a closed inner volume of 90.8 mL. The NaN_3/Al/CuO composite powders were ignited by a tungsten hot-wire. The generated gas was rapidly delivered to a small airbag installed at the end of the gas generator.

The burn rates and ignition delay times of the composite powders were monitored using a high-speed camera (Photron, FASTCAM SA3 120 K) at a frame rate of 5 kHz installed on the benchtop. The high-speed camera used in this study had a minimum and maximum frame rate of 60 and 1 200 000 fps, respectively, sensor of 17.4 mm × 17.4 mm CMOS image sensor, pixel size of 17 μm × 17 μm, and operating voltage and current of AC 100−240 V and 60 A, respectively.

The explosive force was measured using a pressure cell tester system, in which the pressure generated by the thermal ignition of the NaN_3/Al/CuO composites was automatically measured by a pressure sensor (PCB Piezotronics, Model No. 113AO3). The distance between the NaN_3/Al/CuO composite and pressure sensor was ∼2 cm. The pressure was amplified by in-line charge amplifiers (Model No. 422E11, PCB Piezotronics) and transformed into an electric signal by a signal conditioner (Model No. 480C02, PCB Piezotronics) with the frequency response of 25 kHz. This signal was recorded by an oscilloscope (Tektronix, Model No. TDS 2012B). Approximately 13 mg NaN_3/Al/CuO composite powder was placed in the pressure cell tester, and the tungsten hot-wire connected to a power transformer was inserted. The pressure cell was completely sealed, and then voltage was applied. The tungsten hot-wire was rapidly heated and the loaded composite powder was ignited. After pressure was generated by the explosion and gas evolution of the composite powder within the pressure cell, the converted electrical signal was recorded in situ in terms of the time-to-pressure graph in the oscilloscope.

The composite powders fabricated in this study were characterized by various techniques including scanning electron microscopy (SEM; Model Hitachi FE-SEM S-4700, Hitachi, Ltd.) operated at 15 kV, powder X-ray diffractometry (XRD; Model Empyrean Series 2, PANalytical, Ltd.) using Cu Kα radiation, and differential scanning calorimetry (DSC; Model Labsys TGA-DSC/DTA evo, Setaram, Ltd.) performed from 30 to 1000 °C at 10 °C/min under N_2 flow.

DOI: 10.1021/acsami.6b00070
ACS Appl. Mater. Interfaces 2016, 8, 9405−9412

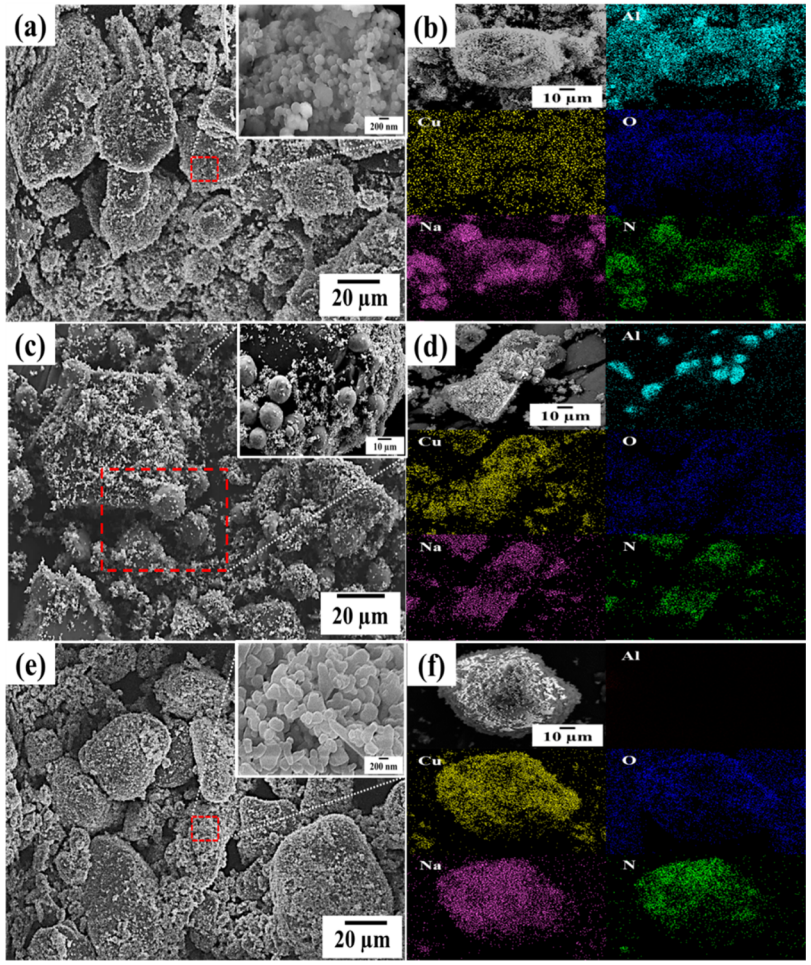

Figure 2. SEM and EDX images of (a, b) NaN_3 MP/Al NP/CuO NP, (c, d) NaN_3 MP/Al MP/CuO NP, and (e, f) NaN_3 MP/CuO NP.

Composite powder	Snapshot	Ignition delay time (ms)	Burn rate (m/s)
NaN_3 MP/ CuO NP	0 ms 6.1 ms 12.2 ms 18.3 ms 24.4 ms	30.6	0.3
NaN_3 MP/ Al MP/ CuO NP	0 ms 4.3 ms 8.6 ms 12.9 ms 17.2 ms	4.2	1.5
NaN_3 MP/ Al NP/ CuO NP	0 ms 0.4 ms 0.8 ms 1.2 ms 1.6 ms	0.6	5.3

Figure 3. Snapshots, ignition delay times, and burn rates of tungsten hot-wire-ignited NaN_3 MP/CuO NP, NaN_3 MP/Al MP/CuO NP, and NaN_3 MP/Al NP/CuO NP composite powders.

3. RESULTS AND DISCUSSION

Figure 2 shows the SEM and EDX images of three different NaN_3/Al/CuO composite powders prepared by the sonication process. The SEM and EDX images in Figure 2a,b show the NaN_3 MP/Al NP/CuO NP composite powder, in which Al NPs and CuO NPs are strongly bound to the surface of the NaN_3 MPs. The inset of Figure 2a depicts a high-resolution SEM image of the Al NPs and CuO NPs covering the surfaces of the NaN_3 MPs. The SEM and EDX images in Figure 2c,d show the NaN_3 MP/Al MP/CuO NP composite powder, in which the Al MPs and CuO NPs are strongly bound to the surface of NaN_3 MPs. The inset of Figure 2c is a high-resolution SEM image showing the Al MPs and CuO NPs covering the surfaces of the NaN_3 MPs. The SEM and EDX images in Figure 2e,f show the NaN_3 MP/CuO NP composite without Al particles, in which CuO NPs are strongly bound to the surfaces of the NaN_3 MPs. The inset of Figure 2e also indicates that the CuO NPs are strongly bound to the surfaces

DOI: 10.1021/acsami.6b00070
ACS Appl. Mater. Interfaces 2016, 8, 9405−9412

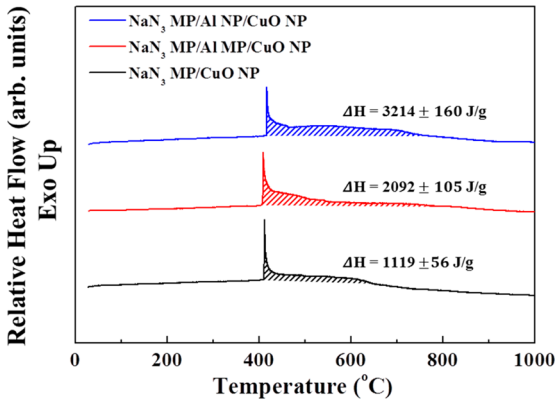

Figure 4. Differential scanning calorimetry (DSC) results of NaN_3 MP/CuO NP, NaN_3 MP/Al MP/CuO NP, and NaN_3 MP/Al NP/CuO NP composite powders.

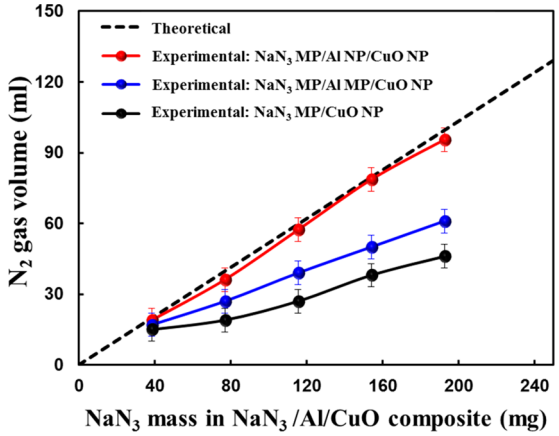

Figure 5. Comparison of theoretically determined N_2 gas volume generated with experimentally determined N_2 gas volume generated by the ignition and combustion reactions of the NaN_3 MP/CuO NP, NaN_3 MP/Al MP/CuO NP, and NaN_3 MP/Al NP/CuO NP composite powders.

of the NaN_3 MPs. These SEM and EDX analyses suggest that the Al MPs, Al NPs, and CuO NPs are homogeneously deposited on the surfaces of the NaN_3 MPs by the simple sonication process employed in this study.

The effect of presence and size of Al particles as heat energy sources on the ignition and combustion characteristics of the NaN_3 MP/CuO NP composite powder was examined. Figure 3 depicts snapshots taken by the high-speed camera after the ignition of the three different composite powders aligned into squares of 8 mm × 8 mm.

Here, the ignition delay time was defined by the time between the moment of direct contact with the hot-wire and the initial ignition of the aligned composite powder. The burn rate was defined as the total length of the aligned powder sample divided by the total time necessary for the flame to propagate from one end to the other of the powder sample. As shown in Figure 3, all three composite powders are successfully ignited and the flame initiated by the hot wire is continuously propagated. The ignition delay times were observed to be ~30.6 ms for NaN_3 MP/CuO NP, ~4.2 ms for NaN_3 MP/Al MP/CuO NP, and ~0.6 ms for NaN_3 MP/Al NP/CuO NP. This suggests that the presence of Al NP in the NaN_3/CuO composite powder can reduce ignition time because the reactivity of the Al NPs is much greater than that of the Al

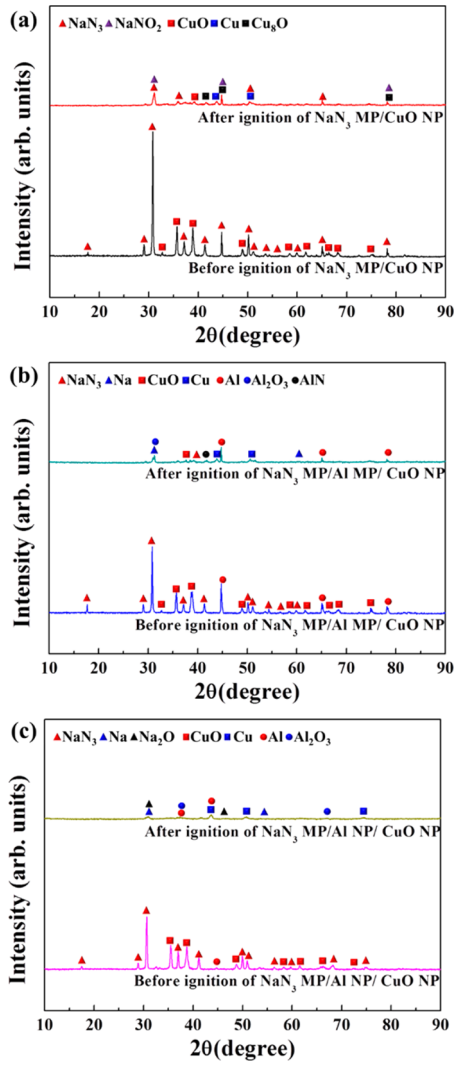

Figure 6. XRD analyses for (a) NaN_3 MP/CuO NP, (b) NaN_3 MP/Al MP/CuO NP, and (c) NaN_3 MP/Al NP/CuO NP composite powders before and after thermal ignition and subsequent combustion reaction.

MPs. This is corroborated by observing the burn rate characteristics. The burn rates of the composite powders are ~0.3 m/s for NaN_3 MP/CuO NP, ~1.5 m/s for NaN_3 MP/Al MP/CuO NP, and ~5.3 m/s for NaN_3 MP/Al NP/CuO NP. This demonstrates that the presence of Al particles in the NaN_3 MP/CuO NP matrix enhances the combustion reaction because the fuel metal of Al generates heat energy, which is rapidly propagated to the adjacent reactive materials. This self-propagating combustion is accelerated the most by adding Al NPs to the NaN_3 MP/CuO NP matrix, because the high specific surface area and reactivity of the Al NPs provide the most effective heat source for triggering fast combustion reactions among the tested NaN_3/CuO composite materials.[38]

The effect of the presence and size of Al particles on the heat energy generation of the NaN_3 MP/CuO NP matrix is corroborated by DSC analysis, as shown in Figure 4. The three samples are initiated at ~400 °C, which approaches the thermal decomposition temperature of NaN_3.[21,22,39] The exothermic reaction of Al and CuO occurs continuously in the range of 550−700 °C. The total heat energy, determined by integrating the positive exothermic heat flow curves, is ~1119 ± 56 J/g for NaN_3 MP/CuO NP, ~2092 ± 105 J/g for NaN_3

DOI: 10.1021/acsami.6b00070
ACS Appl. Mater. Interfaces 2016, 8, 9405−9412

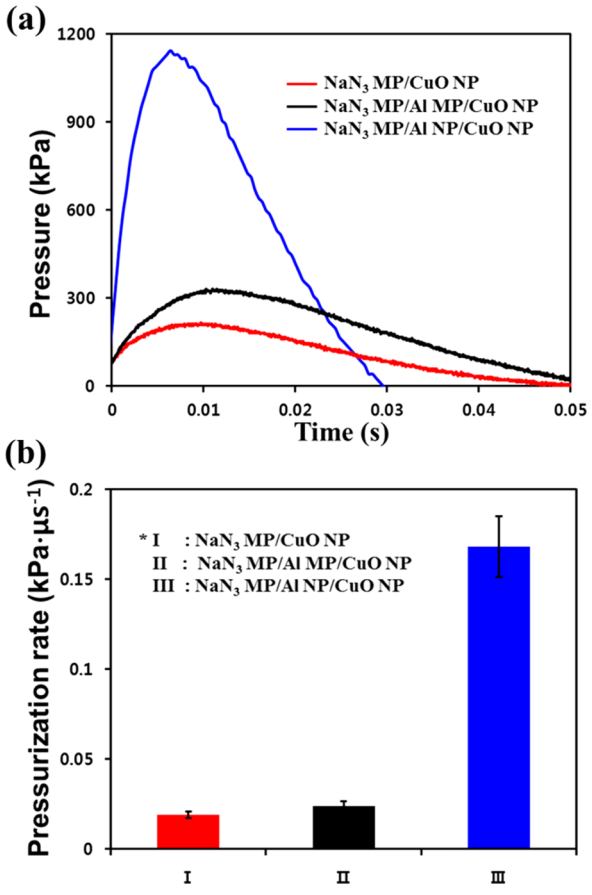

Figure 7. Comparison of (a) pressure traces and (b) pressurization rate of NaN_3 MP/CuO NP, NaN_3 MP/Al MP/CuO NP, and NaN_3 MP/Al NP/CuO NP composite powders.

MP/Al MP/CuO NP, and ~3214 ± 160 J/g for NaN_3 MP/Al NP/CuO NP. These results confirm that the presence of Al in the NaN_3/CuO matrix increases the total heat energy generated by reacting aluminothermically. The addition of Al NPs significantly increases the total heat energy generated from the NaN_3 MP/CuO NP composite powder, suggesting that the Al NPs are more effective heat sources for enhancing the exothermic reaction than the Al MPs are, because of the increased reactivity permitted by the reduced particle size.[40−42] We also performed TGA analyses for all three different samples (i.e., NaN_3 MP/Al NP/CuO NP, NaN_3 MP/Al MP/CuO NP, and NaN_3 MP/CuO NP) to compare the thermal decomposition and the weight change as a function of temperature. As shown in Figure S3 (Supporting Information), there were commonly sharp decreases in weight at ~400 °C, which was similarly observed in the DSC results (Figure 4). In addition, the initial weight was significantly decreased in the order of NaN_3 MP/Al NP/CuO NP > NaN_3 MP/Al MP/CuO NP > NaN_3 MP/CuO NP. These results confirm that the presence of Al in the NaN_3/CuO matrix increases the total heat energy generated by reacting aluminothermically. The addition of Al NPs significantly increases the total heat energy generated from the NaN_3 MP/CuO NP composite powder, suggesting that the Al NPs are more effective heat sources for enhancing the exothermic reaction than the Al MPs are, because of the increased reactivity permitted by the reduced particle size.

The amount of N_2 gas generated by the three different composite powders was experimentally determined by a water substitution method. The experimental data for the N_2 gas generation volume as a function of NaN_3 mass in the NaN_3/Al/CuO composites are compared with the theoretically determined values in Figure 5.

The gas generator was first sealed and the tungsten hot-wire was used to ignite the NaN_3/CuO/Al composite powders installed in the gas generator. As the amount of NaN_3 increases in the composite powders, the volume of evolved N_2 gas is linearly increased both with and without Al particles in the NaN_3 MP/CuO NP matrix, as expected. The volume of N_2 gas generated from the NaN_3 MP/CuO NP composite powders is lower than the theoretical value, because the thermal decomposition of the NaN_3 MPs is incomplete without the Al heat source. The N_2 gas volume is clearly increased by the addition of Al MPs in the NaN_3 MP/CuO NP matrix, suggesting that the ignition and combustion of the Al MP/CuO NP composite provides more heat energy to promote the thermal decomposition of the NaN_3 MPs. The volume of N_2 gas increases further, approaching the theoretical values, when Al NPs are added to the NaN_3 MP/CuO NP matrix, which suggests that the Al NPs are important in generating sufficient heat energy for completing the thermal decomposition of the NaN_3 MPs.

To examine the reactants and byproducts of the thermal reaction of the NaN_3/CuO/Al composite powders, a series of XRD analyses were performed before and after the ignition and combustion reactions of the powders. The possible chemical reaction pathways regarding the three major reactants of NaN_3, Al, and CuO can be represented as follows:[3,19,36,37]

$$2NaN_3 \rightarrow 2Na + 3N_2(g) \quad (1)$$

$$2Al + 3CuO \rightarrow Al_2O_3 + 3Cu \quad (2)$$

$$2Na + CuO \rightarrow Na_2O + Cu \quad (3)$$

First, the NaN_3 MP/CuO NP composite powder experienced a phase change, following the reaction pathways of 1 and 3, after the ignition and combustion reaction. We expected to observe the presence of Cu and Na_2O after the combustion reaction. However, CuO and NaN_3 remains and $NaNO_2$ is found in the reaction products, as shown in Figure 6a. After the ignition of NaN_3 MP/Al MP/CuO NP composite powder, the formation of Al_2O_3, Na, and Cu occurs as shown in Figure 6b. However, NaN_3, CuO, and Al are also observed, indicating that the addition of Al MPs to the NaN_3 MP/CuO NP composite powder provides insufficient heat energy to completely thermally decompose the gas-generating agent.

For the case of the NaN_3 MP/Al NP/CuO NP composite powder, Na, Cu, Na_2O, and Al_2O_3 phases are observed as byproducts of the ignition and combustion reaction, as shown in Figure 6c, which confirms that the addition of Al NPs to the NaN_3 MP/CuO NP composite powders effectively provides sufficient heat energy to complete the thermal decomposition and chemical reaction of the composite. This also suggests that the use of highly reactive Al NPs as fuel sources enables a significant increase in the interfacial contact area among the reactants, and thus the aluminothermic reaction is actively promoted to enhance the reactivity of the components.

Figure 7a shows the pressure traces of the three reactant mixtures ignited in the closed pressure-cell tester system. When Al NPs are added to the NaN_3 MP/CuO NP composites, the magnitude of the pressure rise is 3.5 and 5.4 times greater than that of the pressure generated by the ignition of the NaN_3 MP/

DOI: 10.1021/acsami.6b00070
ACS Appl. Mater. Interfaces 2016, 8, 9405−9412

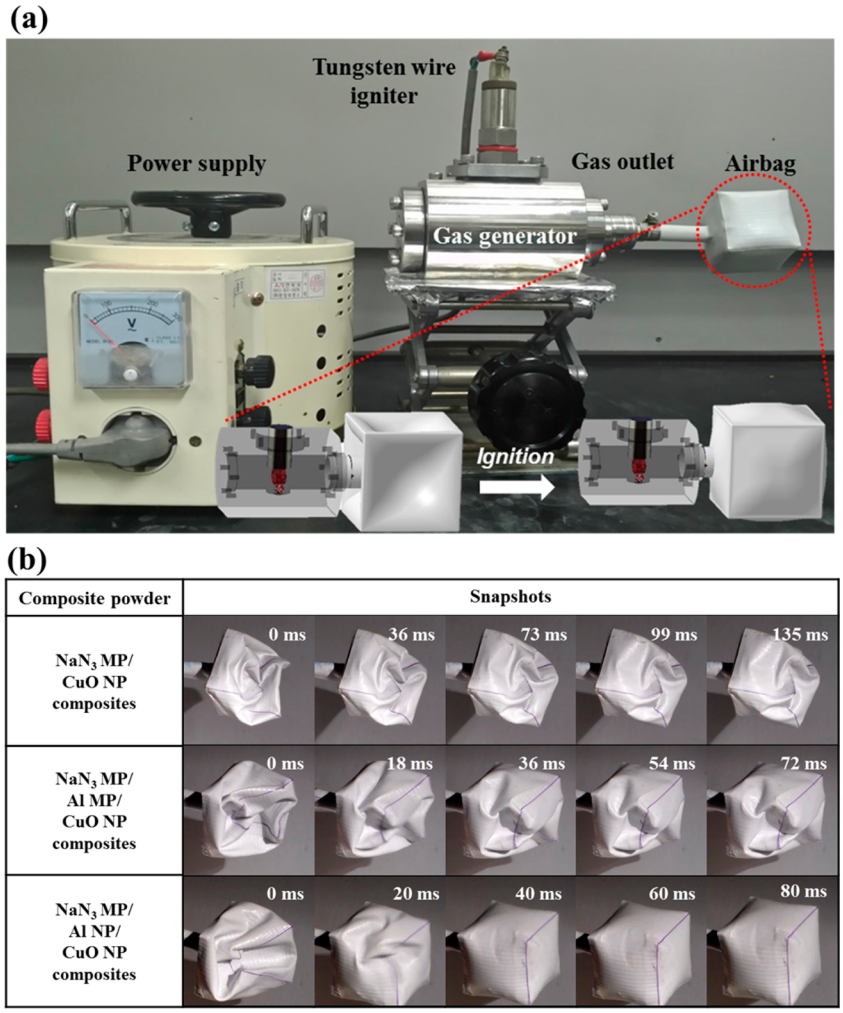

Figure 8. (a) Photograph of small airbag inflation system with schematic of implementation, (b) snapshots of small airbags inflated by ignition and combustion reaction of (i) NaN_3 MP/CuO NP composite powder (partial inflation), (ii) NaN_3 MP/Al MP/CuO NP composite powder (partial inflation) and NaN_3 MP/Al NP/CuO NP composite powder (full inflation).

Al MP/CuO NP and NaN_3 MP/CuO NP composite, respectively. This suggests that the thermal decomposition of the NaN_3 MP is effectively triggered by the heat source of the Al NP-based composites, such that the volume expansion occurs rapidly. Figure 7b shows the pressurization rate, which is determined by calculating the ratio of the maximum pressure to the rise time. Steeper slopes in the time-pressure graphs indicate larger pressurization rates. The NaN_3 MP/CuO NP composite powder without Al particles has the lowest pressure and pressurization rate. The NaN_3 MP/CuO NP composite powder with Al MPs has a slightly higher maximum pressure and pressurization rate, indicating that the presence of Al MPs are not fully effective in generating heat for the thermally decomposition of NaN_3 MPs in the composites. The NaN_3 MP/Al NP/CuO NP composite powder has the highest pressure and pressurization rate, suggesting that a rapid thermal decomposition of NaN_3 is effectively achieved by the presence of highly reactive Al NPs.

The potential application of gas generators installed with NaN_3 MP/CuO NP, NaN_3 MP/Al MP/CuO NP, and NaN_3 MP/Al NP/CuO NP composite powders was observed for the inflation of small airbags, as shown in Figure 8a. The three composite powders were ignited using a tungsten wire in the gas generator, and then the airbags expanded by the gaseous products of the combustion reactions of the composites. Figure 8b shows the snapshots of airbag expansion for the three tested powders. The time until each airbag reaches full expansion is observed to be ~135 ms for NaN_3 MP/CuO NP, ~72 ms for NaN_3 MP/Al MP/CuO NP, and ~40 ms for NaN_3/Al NP/CuO NP. In addition, the airbag inflation rates were ~0.6 L/s for NaN_3 MP/CuO NP powder, ~1.4 L/s for NaN_3 MP/Al MP/CuO NP powder, and ~3.9 L/s for NaN_3/Al NP/CuO NP powder.

Here, the airbag inflation rate is obtained by calculating the ratio of the maximum amount of gas generation to the time required to fill the airbag. The gas generators filled with NaN_3 MP/CuO NP and NaN_3 MP/Al MP/CuO NP composite powders achieved incomplete airbag expansion because the volume of N_2 gas generated by the combustion of reactants was insufficient. Notably, full airbag expansion was only achieved by the NaN_3 MP/Al NP/CuO NP composite within ~40 ms, suggesting that the designed volume of N_2 gas was rapidly generated by the strong aluminothermic reaction occurring because of the presence of nanoscale energetic materials in the form of Al NPs in the NaN_3 MP/CuO NP composites. This confirms that nanoscale Al fuel is much more effective than microscale Al fuel to obtain sufficient gas-generating properties by decomposing NaN_3 in the gas generator.

DOI: 10.1021/acsami.6b00070
ACS Appl. Mater. Interfaces 2016, 8, 9405−9412

4. CONCLUSIONS

In this work, we examined the effect of the presence and size of Al particles as heat energy sources on the combustion and gas-generating properties of NaN_3 MP/CuO NP composite powders, which were used as gas-generating agents/oxidizers, respectively, for gas generators. The NaN_3 MP/Al NP/CuO NP composite powders showed the highest exothermic energy and fastest gas-generating properties of the tested composite powders. This suggests that the use of highly reactive Al NPs as fuel sources in the NaN_3 MP/CuO NP matrix enabled a significantly increase in the interfacial contact area among the reactants, and thus the aluminothermic reaction occurred effectively and significantly enhanced the combustion reactivity of the gas-generating and oxidizing agents. Finally, the full expansion of a small airbag in less than ~40 ms was successfully demonstrated by employing Al NPs in a NaN_3 MP/CuO NP composite fuel installed in the gas generator, suggesting that the rapid, stable, and complete thermal decomposition of NaN_3 MP/CuO NP composites can be effectively achieved by employing Al NPs of high reactivity.

■ ASSOCIATED CONTENT

Supporting Information

The Supporting Information is available free of charge on the ACS Publications website at DOI: 10.1021/acsami.6b00070.

SEM/TEM images and particle size distributions, low- and high-resolution TEM images of Al NPs and Al MPs, and thermogravimetric analysis results (PDF).

■ AUTHOR INFORMATION

Corresponding Author

*E-mail: sookim@pusan.ac.kr (S. H. Kim).

Author Contributions

Both S. B. Kim and K. J. Kim equally contributed to this work as first authors.

Notes

The authors declare no competing financial interest.

■ ACKNOWLEDGMENTS

This research was supported by the Civil & Military Technology Cooperation Program through the National Research Foundation of Korea (NRF) funded by the Ministry of Science, ICT & Future Planning (No. 2013M3C1A9055407). This research was also partially supported by the Fundamental Research Program funded by the Agency for Defense Development of Korea (No. UD130033GD).

■ REFERENCES

(1) King, W. P.; Saxena, S.; Nelson, B. A.; Weeks, B. L.; Pitchimani, R. Nanoscale Thermal Analysis of an Energetic Material. *Nano Lett.* **2006**, *6*, 2145−2149.

(2) Shende, R.; Subramanian, S.; Hasan, S.; Apperson, S.; Thiruvengadathan, R.; Gangopadhyay, K.; Gangopadhyay, S.; Redner, P.; Kapoor, D.; Nicolich, S.; Balas, W. Nanoenergetic Composites of CuO Nanorods, Nanowires, and Al-Nanoparticles. *Propellants, Explos., Pyrotech.* **2008**, *33*, 122−130.

(3) Ahn, J. Y.; Kim, J. H.; Kim, J. M.; Lee, D. W.; Park, J. K.; Lee, D.; Kim, S. H. Combustion Characteristics of High-Energy Al/CuO Composite Powders: The Role of Oxidizer Structure and Pellet Density. *Powder Technol.* **2013**, *241*, 67−73.

(4) Jian, G.; Feng, J.; Jacob, R. J.; Egan, G. C.; Zachariah, M. R. Super-Reactive Nanoenergetic Gas Generators Based on Periodate Salts. *Angew. Chem., Int. Ed.* **2013**, *52*, 9743−9746.

(5) Zhou, X.; Torabi, M.; Lu, J.; Shen, R.; Zhang, K. Nanostructured Energetic Composites: Synthesis, Ignition/Combustion Modeling, and Applications. *ACS Appl. Mater. Interfaces* **2014**, *6* (5), 3058−3074.

(6) Weismiller, M. R.; Malchi, J. Y.; Lee, J. G.; Yetter, R. A.; Foley, T. J. Effects of Fuel and Oxidizer Particle Dimensions on the Propagation of Aluminum Containing Thermites. *Proc. Combust. Inst.* **2011**, *33*, 1989−1996.

(7) Kim, J. H.; Ahn, J. Y.; Park, H. S.; Kim, S. H. Optical Ignition of Nanoenergetic Materials: The Role of Single-Walled Carbon Nanotubes as Potential Optical Igniters. *Combust. Flame* **2013**, *160*, 830−834.

(8) Ahn, J. Y.; Kim, J. Y.; Kim, J. M.; Kim, S. H.; Lee, D. W.; Park, J. K. Effect of Oxidizer Nanostructures on Propulsion Forces Generated by Thermal Ignition of Nano-Aluminum-based Propellants. *J. Nanosci. Nanotechnol.* **2013**, *13*, 7037−7041.

(9) Dreizin, E. L. Metal-based Reactive Nanomaterials. *Prog. Energy Combust. Sci.* **2009**, *35*, 141−167.

(10) Blobaum, K. J.; Reiss, M. E.; Plitzko, J. M.; Weihs, T. P. Deposition and Characterization of a Self-Propagating CuO_x/Al Thermite Reaction in a Multilayer Foil Geometry. *J. Appl. Phys.* **2003**, *94*, 2915−2922.

(11) Cheng, J. L.; Hng, H. H.; Ng, H. Y.; Soon, P. C.; Lee, Y. W. Synthesis and Characterization of Self-Assembled Nanoenergetic Al-Fe_2O_3 Thermite System. *J. Phys. Chem. Solids* **2010**, *71*, 90−94.

(12) Son, S. F.; Asay, B. W.; Foley, T. J.; Yetter, R. A.; Wu, M. H.; Risha, G. A. Combustion of Nanoscale Al/MoO_3 Thermite in Microchannels. *J. Propul. Power* **2007**, *23*, 715−721.

(13) Ahn, J. Y.; Kim, W. D.; Cho, K.; Lee, D.; Kim, S. H. Effect of Metal Oxide Nanostructures on the Explosive Property of Metastable Intermolecular Composite Particles. *Powder Technol.* **2011**, *211*, 65−71.

(14) Kim, S. H.; Zachariah, M. R. Enhancing the Rate of Energy Release from Nanoenergetic Materials by Electrostatically Enhanced Assembly. *Adv. Mater.* **2004**, *16*, 1821−1825.

(15) Malchi, J. Y.; Foley, T. J.; Yetter, R. A. Electrostatically Self-Assembled Nanocomposite Reactive Microspheres. *ACS Appl. Mater. Interfaces* **2009**, *1* (11), 2420−2423.

(16) Pagoria, P. F.; Lee, G. S.; Mitchell, A. R.; Schmidt, R. D. A Review of Energetic Materials Synthesis. *Thermochim. Acta* **2002**, *384*, 187−204.

(17) Butler, P. B.; Kang, J.; Krier, H. Modeling and Numerical Simulation of the Internal Thermochemistry of Automotive Airbag Inflators. *Prog. Energy Combust. Sci.* **1993**, *19*, 365−382.

(18) Garner, E. F.; Calif, S. Low Temperature Gas Generator Propellant. U.S. Patent 3,912,562, October 14, 1975.

(19) Yinsheng, H.; Shizhi, D.; Tongju, S.; Ruiqi, S.; Yinghua, Y. Thermal Analysis of Aodium Azide and Its Mixtures. *Thermochim. Acta* **1996**, *284*, 441−444.

(20) Said, A. A.; Alqasimi, R. Thermal Decomposition of Sodium Azide Catalyzed by NiO-Co_3O_4 Solids. *J. Mater. Sci. Lett.* **1992**, *11*, 266−268.

(21) Potvin, H.; Back, M. H. A Study of the Decomposition of Sodium Azide Using Differential Thermal Analysis. *Can. J. Chem.* **1973**, *51*, 183−186.

(22) Hasue, K.; Iwama, A.; Kazumi, T. Combustion Aspects of Sodium Azide and Its Mixtures with Potassium Perchlorate and Burning Catalysts. *Propellants, Explos., Pyrotech.* **1991**, *16*, 245−252.

(23) Khandhadia, P. S.; Burns, S. P. Thermally Stable Nonazide Automotive Airbag Propellants. U.S. Patent 6,306,232, October 23, 2001.

(24) Gast, E.; Schmid, B.; Recker, C.; Walz, S.; Mayr, T.; Semmler, P. Gas Generator Fuel Composition. U.S. Patent 2004/0108031, Jun 10, 2004.

(25) Date, S.; Sugiyama, T.; Itadzu, N.; Nishi, S. Burning Characteristics and Sensitivity Characteristics of Some Guanidium 1,

DOI: 10.1021/acsami.6b00070
ACS Appl. Mater. Interfaces 2016, 8, 9405−9412

5′-bis-1-H-tetrazolate/Metal Oxide Mixtures as Candidate Gas Generating Agent. *Propellants, Explos., Pyrotech.* **2011**, *36*, 51−56.
(26) Chavez, D. E.; Hiskey, M. A. 1, 2, 4, 5- Tetrazine Based Energetic Materials. *J. Energ. Mater.* **1999**, *17*, 357−377.
(27) Klapotke, T. M.; Piercey, D. G. 1,1′-Azobis(tetrazole): A Highly Energetic Nitrogen-rich Compound with a N_{10} Chain. *Inorg. Chem.* **2011**, *50*, 2732−2734.
(28) Pietz, J. F. Method and Composition for Generating Nitrogen Gas. U.S. Patent 3,895,098, July 15, 1975.
(29) Hirata, N.; Matsuda, N.; Kubota, N. Combustion of NaN_3 Based Energetic Pyrolants. *Propellants, Explos., Pyrotech.* **2000**, *25*, 217−219.
(30) Ramaswamy, C. P.; Grzelczyk, C. Gas Generating Composition. U.S. Patent 5,661,261, August 26, 1997.
(31) Madlung, A. The Chemistry Behind Aigbag. *J. Chem. Educ.* **1996**, *73*, 347−348.
(32) Willams, G. K.; Burns, S. P.; Halpin, J. W.; Khandhadia, P. S. Nonazide Gas Generant. U.S. Patent 6,887,326, May 3, 2005.
(33) Mendenhall, I. V.; Taylor, R. D. Gas Generation with Copper Complexed Imidazole and Derivatives. U.S. Patent 7,470,337, December 30, 2008.
(34) Mengmeng, W.; Zhiming, D.; Taiwen, X. Analysis and Purification of the Combustion Gas of Gas Generant. *Procedia Eng.* **2014**, *84*, 826−833.
(35) Mendenhall, I. V.; Barnes, M. W. Burn Rate Enhancement via a Transition Metal Complex of Diammonium Bitetrazole. U.S. Patent 6,712,918, March 30, 2004.
(36) Ulas, A.; Risha, G. A.; Kuo, K. K. An Investigation of the Performance of a Boron/Potassium Nitrate Based Pyrotechnic Igniter. *Propellants, Explos., Pyrotech.* **2006**, *31*, 311−317.
(37) Pashechko, M. I.; Vasiliv, Kh. B.; Rudkovskii, E. M. Thermodynamics of Processes Occurring During the Application of Coatings by Hot Metallization. *Powder Metall. Met. Ceram.* **1997**, *36*, 614−620.
(38) Galfetti, L.; Deluca, L. T.; Severini, F.; Colombo, G.; Meda, L.; Marra, G. Pre and Post-Burning Analysis of Nano-Aluminized Solid Rocket Propellants. *Aerosp. Sci. Technol.* **2007**, *11*, 26−32.
(39) Eslami, A.; Ghorban, H.; Asadi, V. The Effect of Micro-encapsulation with Nitrocellulose on Thermal Properties of Sodium Azide Particles. *Prog. Org. Coat.* **2009**, *65*, 269−274.
(40) Plantier, K. B.; Pantoya, M. L.; Gash, A. E. Combustion Wave Speeds of Nanocomposite Al/Fe_2O_3: The Effects of Fe_2O_3 Particle Synthesis Technique. *Combust. Flame* **2005**, *140*, 299−309.
(41) Pantoya, M. L.; Granier, J. J. Combustion Behavior of Highly Energetic Thermites: Nano versus Micron Composites. *Propellants, Explos., Pyrotech.* **2005**, *30*, 53−62.
(42) Watson, K. W.; Pantoya, M. L.; Levitas, V. I. Fast Reactions with Nano- and Micrometer Aluminum: A Study on Oxidation versus Fluorination. *Combust. Flame* **2008**, *155*, 619−634.

DOI: 10.1021/acsami.6b00070
ACS Appl. Mater. Interfaces 2016, 8, 9405−9412